Proc. Estonian Acad. Sci. Phys. Math., 2004, **53**, 1, 26–44
https://doi.org/10.3176/phys.math.2004.1.03

Nonlinear and scale-invariant analysis of heart rate variability

Jaan Kalda[a], Maksim Säkki[a], Meelis Vainu[b], and Mari Laan[c]

[a] Institute of Cybernetics at Tallinn Technical University, Akadeemia tee 21, 12618 Tallinn, Estonia; kalda@ioc.ee
[b] Tallinn Diagnostic Centre, Suur-Ameerika 18, 10122 Tallinn, Estonia
[c] Tallinn Children Hospital, Tervise 28, 13419 Tallinn, Estonia

Received 11 March 2003, in revised form 6 August 2003

Abstract. Human heart rate fluctuates in a complex and nonstationary manner. Elaborating efficient and adequate tools for the analysis of such signals has been a great challenge for the researchers during last decades. Here, an overview of the main research results in this field is given. The following questions are addressed: What are the intrinsic features of the heart rate variability signal? What are the most promising nonlinear measures, bearing in mind clinical diagnostic and prognostic applications?

Key words: heart rate variability, nonlinear time-series, intermittency.

1. INTRODUCTION

The heart rate of healthy subjects fluctuates in a complex manner. These nonstationary and nonlinear fluctuations are related mainly to a nonlinear interaction between competing neuroautonomic inputs: parasympathetic input decreases and sympathetic stimulation increases the heart rate. Meanwhile, heart pathologies may decrease the responsiveness of the heart and lead to a failure to respond to the external stimuli. Evidently, such pathologies lead to an overall reduction of heart rate variability (HRV). Understanding the diagnostic and prognostic significance of the various measures of HRV has great importance for the cardiology as a whole, because unlike the invasive methods of diagnostics, the required measurements are low-cost and harmless for patients. A particularly important application is the prognostics of the patients with increased risk of sudden cardiac death. While the “linear measures” of HRV are nowadays widely used in clinical practice, the

importance of more complicated measures has been hotly disputed in the scientific literature during the recent decades.

The structure of this review is as follows. In Section 2, general aspects of the heart rate generation, electrocardiogram (ECG) structure, and data acquisition are discussed. In Section 3, we give a brief overview of the "linear era" of the HRV analysis. Section 4 is devoted to the early studies of the nonlinearity of HRV, i.e. to the methods based on the reconstructed phase-space analysis. Here we also provide the modern view on the applicability of these methods. In Section 5, we discuss the self-affine and multi-affine aspects of HRV (including the wavelet-transform-based techniques). Section 6 deals with the phenomenon which can be referred to as "intertwining of low- and high-variability periods". Section 7 examines the effect of synchronization between the heart rate and respiration. Section 8 provides a brief conclusion.

2. HEART RATE GENERATION, ECG, AND DATA ACQUISITION

The quasi-periodic contraction of the cardiac muscle is governed by the electrical signal, which is generated by the sino-atrial (SA) node – a set of electrically active cells in a small area of the right atrium. The signal spreads through the atrial muscle leading to its contraction. It also spreads into a set of specialized cells – the atrio-ventricular (AV) node. Further the signal spreads via the His-Purkinje bundle (which is a fractal-like set of electrically conductive fibres) to the myocardial cells causing their contraction. The ECG is measured as the electrical potential between different points at the body surface. The activity of the SA node by itself is not reflected on the ECG. The electrical activation of the atrial cells leads to the appearance of the P-wave of the ECG. The Q, R, S, and T waves (see Fig. 1) are caused by the electrical activity of the ventricular muscle. The heart rate is generally measured as the RR-interval t_{RR} – the time-lag between two subsequent R-pikes (R-pike itself corresponds to the ventricular contraction). For the HRV analysis, only the normal heart activity is taken into account. All the QRS-complexes are labelled as normal or arrhythmic. Note that even for healthy patients, some heartbeats can be arrhythmic. Normal-to-normal (NN) interval t_{NN} is defined as the value of t_{RR} for such heartbeats, which have both starting and ending R-pikes labelled as normal (see Fig. 1).

Typically, HRV analysis is based on the 24-hour recordings of the *Holter-monitoring*. Shorter ECG recordings can be used for this purpose as well; however, in that case it is impossible to observe the long-scale variations and compare the sleep-awake differences in the heart rhythm. Portable apparatus stores the ECG data as the time-dependent voltage $U(t)$ either on a tape or on a PC flash card; the sampling rate is 125 Hz or higher. The data are later analysed by computer software. Typical commercial software allows visualization of the ECG recording, automated or semiautomated recognition of arrhythmias and artifacts, and the calculation of the standard "linear" characteristics of HRV. Most often, a research

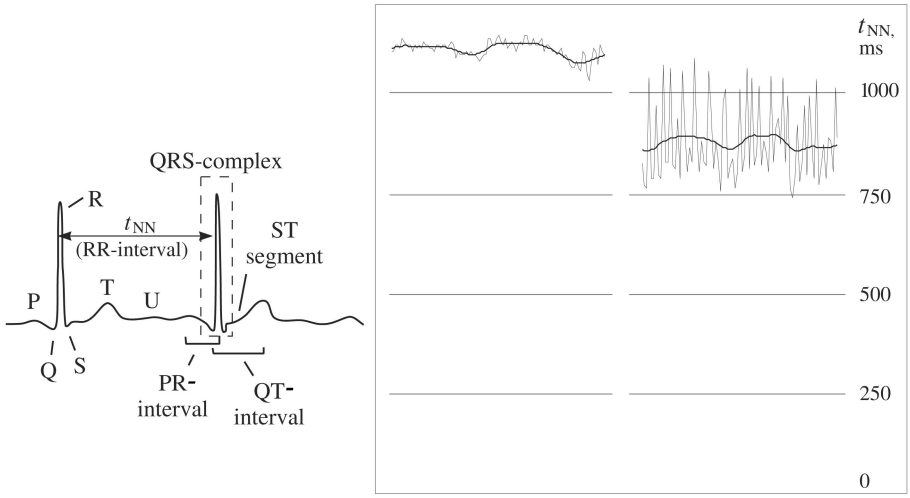

Fig. 1. Left image: normal ECG recording. Image on the right: t_{NN} sequences of low and high variability.

devoted to the methods of nonlinear dynamics is based on plain sequences of NN-intervals and disregards the details of the continuous ECG recordings. Other aspects of the ECG, e.g. the clustering of arrhythmic beats [1] and dynamics of QT intervals [2] (pp. 13–16) are also of high clinical importance, but remain beyond the scope of this review.

The experimental data serving as the basis of the original research performed by the authors of the review were recorded (a) at the Tallinn Nõmme Hospital (children) and (b) Tallinn Diagnostic Centre (adult subjects). The scheme of data acquisition is presented in Fig. 2. For group (a), the recordings of ambulatory Holter-monitoring covered 12 healthy subjects of mean age 11.5 ± 3.3 years, 6

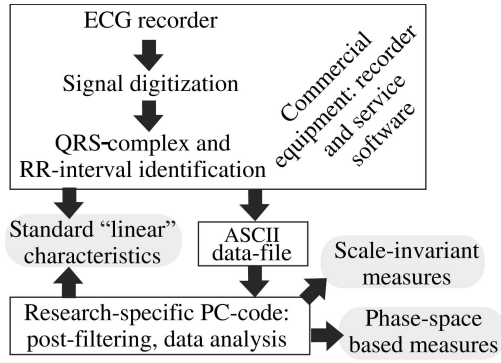

Fig. 2. The analysis of heart rate variability: the scheme of data acquisition and analysis.

Table 1. Test groups of patients. Abbreviations are as follows: IHD – ischemic heart disease (stenocardia); SND – sinus node disease; VES – ventricular extrasystole; PCI – post cardiac infarction; RR – blood pressure disease; FSK – functional disease of sinus node

	Healthy	IHD	SND	VES	PCI	RR	FSK
No. of patients	103	8	11	16	7	11	6
Mean age	45.5	65.4	50.0	55.9	47.3	55.5	11.7
Std. dev. of age	20.5	11.4	19.3	14.3	11.6	14.4	4.6

children with clinically documented sinus node disease (mean age 11.5 ± 1.9 years), and 12 subjects with miscellaneous diagnosis. The sampling rate of the ECG was 125 Hz. For group (b), specifics are given in Table 1. These data have been obtained during regular diagnostical examinations of more than 200 patients using the *Rozinn* equipment; the ECG sampling rate has been 180 Hz. It is known that there can be significant differences between the HRV dynamics of young and adult subjects. The primary goal of including the children groups has been to test the universality (age-independence) of the scaling behaviour of HRV qualitatively. The diagnostics and data verification have been made by a qualified cardiologist. The data preprocessing included filtering out falsely detected QRS-complexes (artifacts and arrhythmias) using the commercial *Rozinn* software.

3. LINEAR MEASURES OF HRV

The clinical importance of HRV was first noted in 1965 by Hon and Lee [3]. Since then, the statistical properties of the interbeat interval sequences have attracted the attention of a wide scientific community. An increased risk of post-infarction mortality was associated with the reduced HRV by Wolf et al. [4] in 1977.

The problem received wider attention in the early 1980s, when Akselrod et al. [5] introduced the spectral methods for the HRV analysis. The spectral characteristics are generally referred to as "frequency-domain characteristics" and are opposed to the "time-domain methods", which are derived directly from the t_{NN}-sequence. In the late 1980s, the clinical importance of HRV became generally recognized. Several studies confirmed that HRV was a strong and independent predictor of mortality following an acute myocardial infarction [6–8]. As a result, a breakthrough has been achieved: the "linear" measures of HRV became important tools of clinical practice.

A nonexhaustive list of the parameters currently used in medical practice is as follows: the mean NN-interval, the difference between night and day heart rate, the longest and shortest NN-intervals, the standard deviation of the NN-interval (SDNN, typically calculated over a 24-hour period), the standard deviation of locally (usually 5 min) averaged NN-intervals (SDANN), the mean of the 5-minute

standard deviation of the NN-interval (averaged over 24 h; SDNN index), the square root of the mean squared differences of successive NN-intervals (RMSSD), the percentage of interval differences of successive NN-intervals greater than 50 ms (pNN50), the spectral power of high- and low-frequency fluctuations in NN-sequences.

4. RECONSTRUCTED PHASE-SPACE

It is widely accepted that the heart rhythm generation in the complex of the sinus node and atrio-ventricular node can be well described by nonlinear dynamical models, where the SA node and AV node form a system of nonlinear coupled oscillators [9−10]. The model has been proven to be viable and predicts several experimentally observed phenomena, such as Wenckebach and Mobitz type II arrhythmias and bistable behaviour [10]. This deterministic nonlinear model predicts that the phase trajectories of an healthy heart lie on an attractor of the coupled system of oscillators. Consequently, one should be able to observe well-defined patterns on the Poincarè sections of the phase-space. Note that in the case of physiological data, there is no information, what might be the canonical variables. Therefore, the phase trajectory is reconstructed in time-delay coordinates $U(t)$, $U(t+\tau)$, ..., $U[t+(D-1)\tau]$ [or $t_{\mathrm{NN}}(n)$, $t(n+1)$, ..., $t(n+D-1)$]. Here D is the so-called embedding dimensionality, i.e. the dimensionality of the reconstructed phase-space. It is expected that the real phase trajectory is mapped to the reconstructed trajectory by a smooth transform.

Exactly such a reasoning has led to the idea that the dynamical characteristics from the theory of nonlinear dynamics could be used for the diagnostic purposes. The early studies by Babloyantz et al. [11] gave rise to extensive studies in the 1990s [12−15]. The experimental observations seemingly confirmed the theoretical expectations. Particularly, the correlation dimension of the continuous ECG recording (i.e. the recorded voltage as a function of time) has been reported to be between 3.6 and 5.2. The conclusion has been that the dynamics of the heart of a healthy person is less regular than that of a person with severe cardiac pathologies. Correspondingly, the correlation dimension has often been thought to be a measure for the healthiness of the heart. The other tools of the analysis of nonlinear dynamical systems (such as Lyapunov exponents; Kolmogorov, Shannon, pattern, and approximate entropies; etc.) have been exploited to an equal extent.

The correlation dimension of a data sequence is typically calculated according to the Grassberger–Procaccia algorithm [16]. In a reconstructed phase-space of dimensionality D, the correlation sum $C = \frac{2}{N(N-1)} \sum_{i,j} \theta(r - |r_i - r_j|)$ is calculated as a function of the radius r; it is expected to behave as a power-law $C \propto r^{\nu(D)}$. Here r_i denotes the D-dimensional radius-vector of the ith data-point, and $\theta(r)$ stands for the Heaviside function. The correlation dimension d_c is found as the limit of ν at large values of D (in fact, it is expected that for $D > d_c$, the exponent ν is independent of D, and in that case $\nu = d_c$).

However, there are various arguments leading us to the conclusion that the formally calculated correlation dimension of a heart rhythm does not correspond to the dimensionality of an intrinsic attractor; similarly, the formally calculated Lyapunov exponents, entropies, etc. do not describe the respective aspects of underlying nonlinear dynamics. First, it has been pointed out that physiological time-series are typically nonstationary and noisy, and therefore, the correlation dimension cannot be calculated reliably [17−19]; this fact is nowadays widely accepted. In the case of the human heart, the "noise" comes from the autonomous nervous system in the form of inputs regulating the heart rate (cf. [20−22]): from the viewpoint of the underlying nonlinear deterministic system, these effectively nondeterministic signals perform the role of high-level noise. It should also be noted that some inputs of the autonomous nervous system may lead to quasi-periodic signals – an easy source of false detection of low-dimensional chaos and apparent patterns in simple time delay maps (see Figs. 3, 4). Thus, respiration gives rise to the signal of a typical period of 4 s; the effect is most pronounced when the patient is at rest, and is stronger for young persons. Second, it has been emphasized that a reasonable fitting of a correlation sum to a power law does not necessarily mean that the obtained exponent is the correlation dimension of the underlying dynamical system; instead, a thorough nonautomatable verification procedure has to be done [23]. Third, the length of the data sequences is often inadequate for reliable calculation of high values of the correlation dimension $d_c \gtrsim 6$, cf. [15,23].

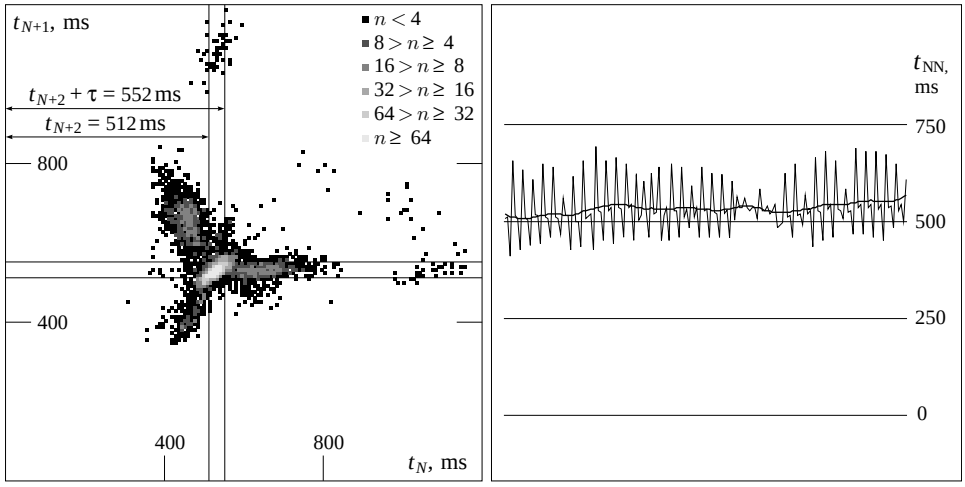

Fig. 3. A cross-section of the 3-dimensional reconstructed phase-space for a patient with pronounced 4:1 mode-locking (see also Section 7); around the central cloud of points, three major satellite-clouds can be seen; these satellite-clouds correspond to the sequence of interbeat intervals, shown on the right-hand plot. The observed oscillations with period 4 can be attributed to the modulation of the heart rate by respiration.

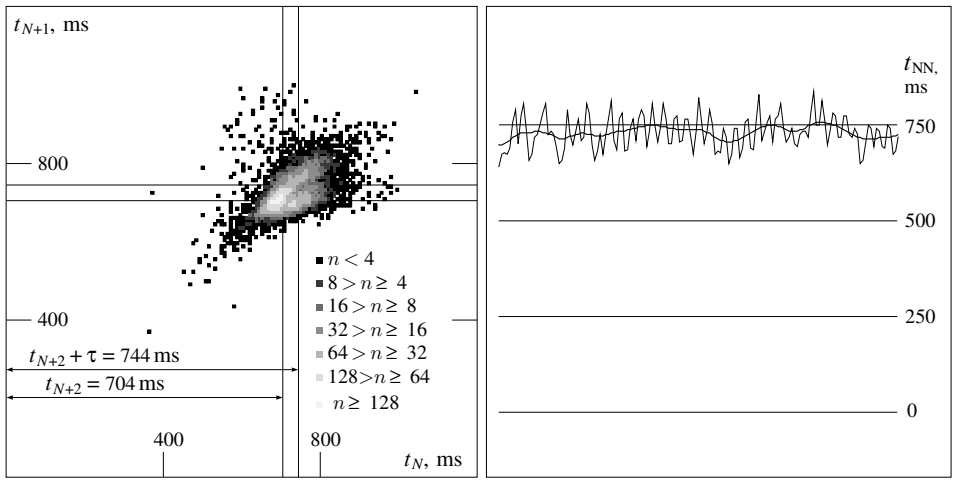

Fig. 4. The same as in Fig. 3. Mode-locking (4:1 and 5:1) is weaker, but the heart rate modulation by the respiration is significant. One can distinguish two branches of the central cloud, which are caused by the respiratory modulation.

The above discussed research results can be summarized as follows: (1) The correlation sums of the human heart rate follow typically a scaling law. (2) In most cases, the scaling exponents are not the correlation dimensions. This leads us to a natural question: what is the physical meaning of these formally calculated exponents? Our answer to this question is based on simple observations, valid for healthy patients: (a) the long-time variability of the interbeat intervals is typically much higher than the variability on the time-scale of few heartbeats; (b) for the periods when the mean heart rate is high (when the subject is performing physical exercise) HRV is low; (c) the heart rate is controlled by effectively random nondeterministic inputs arriving from the autonomous nervous system. As a consequence, in time delay coordinates, an HRV time-series generates a baseball bat-shaped cloud of points. Although the theoretical value of the correlation dimension of such a cloud is infinite, the finite resolution of the recording apparatus, finite length of the time-series, and the linear structure of the cloud result in a smaller value. This is evident for a very narrow "bat", which is efficiently one-dimensional.

Our conjecture passes also a quantitative test: the correlation sum of surrogate data-sets constructed using Gaussian random data-series and mimicking the features (a)–(c) (see Fig. 5) scales almost identically to that of clinical HRV data (see Fig. 6 and [24]).

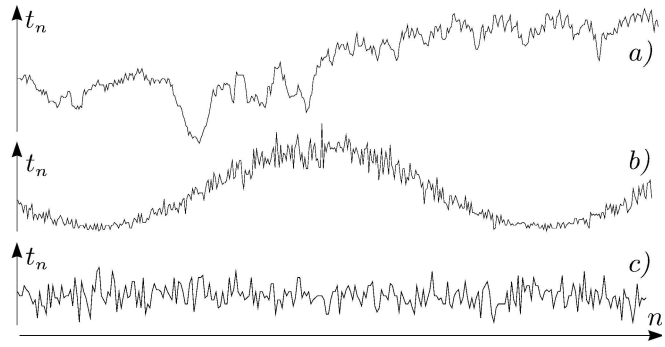

Fig. 5. Time-series for real HRV data (a), surrogate data (b), and Gaussian noise (c); the beat interval t_n is plotted versus the beat number n.

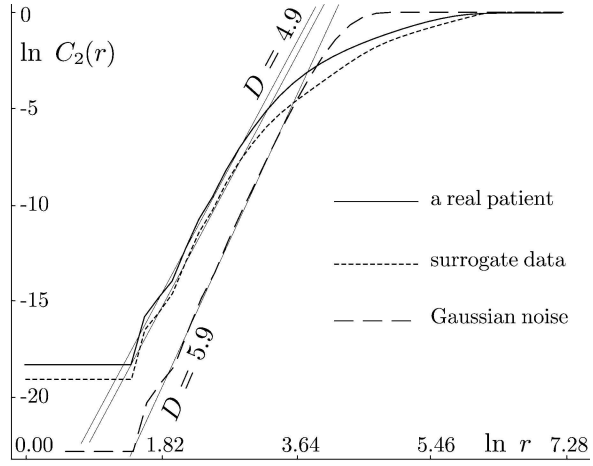

Fig. 6. The correlation sum $C_2(r)$ (as a function of the radius r) of surrogate data scales almost identically to the real clinical data.

To conclude, the measures based on the reconstructed phase-space fail to describe a deterministic chaos inside the heart, because the deterministic dynamics is suppressed by essentially intermittent signals arriving from the autonomous nervous system and regulating the heart rhythm. However, some fine-tuned measures (e.g. various entropies; cf. [25]) can be useful in describing the level of short-time variability of the heart rhythm, and complement the linear quantity pNN50 (which also measures the high-frequency component of HRV).

5. SCALE-INDEPENDENT MEASURES

Recent studies have shown that scale-invariant characteristics can be successfully applied to the HRV analysis [26−29]. However, this conclusion has been disputed, and certain scale-dependent measures (particularly, the amplitude of the wavelet spectra at a specific time-scale) have been claimed to provide better results [30]. The scale-independent methods have been believed to be more universal, subject-independent, and to reflect directly the dynamics of the underlying system, unlike the scale-dependent methods which may reflect characteristics specific to the subject and/or to the method of analysis [29]. The opposing argument has been that certain heart disorders affect HRV at a specific scale or range of scales; owing to this circumstance, at the properly chosen time-scale, scale-dependent measures may provide a useful information [30].

The simplest relevant scale-independent measure is the Hurst exponent H, which has been introduced to describe statistically self-affine random functions $f(r)$ of one or more variables [31]. Such a function is referred to as a *fractional Brownian function* and satisfies the scaling law

$$\left\langle [f(r_1) - f(r_2)]^2 \right\rangle \propto |r_1 - r_2|^{2H}.$$

Note that $H = \frac{1}{2}$ is a special case of ordinary Brownian function – the increments of the function are delta-correlated, and $f(r)$ can be thought to be the displacement of a Brownian particle as a function of time r. Therefore, in the case of $H < \frac{1}{2}$, there is a negative *long-range correlation* between the increments of the function. Analogously, $H > \frac{1}{2}$ corresponds to a positive correlation. Note that the early scale-invariant studies of HRV were based on power spectra [32,33], an aspect closely related to the scaling exponent H.

Many phenomena in nature exhibit this kind of scale-invariance and lead to fractional Brownian time-series [31]. The same is true for HRV: after filtering out short-scale components with $\tau < 30$ s (corresponding to the respiratory rhythm, to the blood-pressure oscillations, and to the pathological Cheyne–Stokes respiration), the fluctuation function $F(n)$, defined as

$$F(\nu) = \langle |t_n - t_{n+\nu}| \rangle \tag{1}$$

revealed a good scaling behaviour $F(\nu) \propto \nu^H$ [26]. While for healthy patients, the increments of the heart rhythm were found to be significantly anticorrelated resulting in $H < \frac{1}{2}$, the heart rhythm of the patients with dilated cardiomyopathy was essentially Brownian with $H \approx \frac{1}{2}$ [26]. In the case of our patient groups, there was no significant correlation between the diagnosis and the Hurst exponent, and there were also ca 7% healthy subjects with $H = 0.5 \pm 0.05$ (cf. Fig. 7 and Table 2).

Finally, various techniques, such as detrended fluctuation analysis [27], detrended time-series analysis [34], and wavelet amplitude analysis [35] have been proposed to fine-tune the Hurst-exponent-based approach.

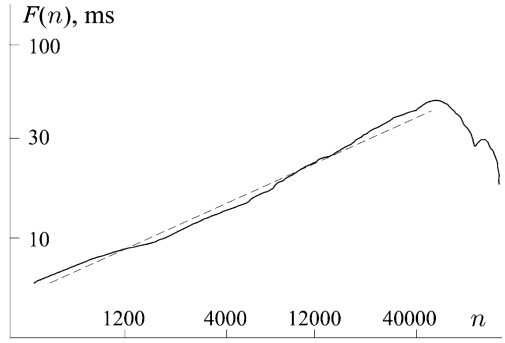

Fig. 7. The fluctuation function $F(\nu)$ is plotted versus the time lag ν. The almost straight line indicates a good scaling behaviour $F(\nu) \propto \nu^H$ (here with $H = 0.50$).

Table 2. For the patient groups of Table 1, the diagnosis and the Hurst exponent *H* values were effectively uncorrelated

	Healthy	IHD	SND	VES	PCI	RR	FSK
Mean value of *H*	0.30	0.28	0.32	0.35	0.29	0.29	0.28
Std. dev. of *H*	0.10	0.09	0.11	0.12	0.12	0.08	0.06

Complex nonstationary time-series cannot be described by a single scaling exponent H. Indeed, simple scaling behaviour is expected if there is a Gaussian distribution of increments. However, even in the case of Gaussian functions, the scaling exponent is not necessarily constant over the whole range of scales. Instead, it can be a slow (e.g. logarithmic) function of the scale, so that other descriptions (such as stretched exponentials) may be required. Physiological time-series are typically non-Gaussian. For such functions, scale-invariance can be very complicated. A nonexhaustive way to describe such a behaviour is to calculate the multifractal spectrum of Hurst exponents [36]. Therefore, it is not surprising that the human heart rate signal was found to obey a multi-affine structure [28,29].

Qualitatively, a multifractal time-series behaves as follows. Each point of the time-series is characterized by its own Hurst exponent h (referred to as the Lipschitz–Hölder exponent); this exponent describes the local scaling of fluctuations. Then, the distribution of points of fixed values of h is self-similar and is described by a fractal dimension $f(h)$. Technically, the spectrum $f(h)$ can be calculated by the means of wavelet transform (cf. [29]). This scheme includes the calculation of the scaling exponents $\tau(q)$ (referred to as the mass exponents), which describe, how the qth moment of the wavelet transform amplitude scales with the wavelet width. The scaling exponents $\tau(2)$ and $\tau(5)$ have been found to have

a significant prognostic value (for the post-infarction prognosis) [29]. The wavelet transform amplitudes, calculated for a specific wavelet width (≈ 5 min) have been claimed to be of even higher prognostic value [30]. However, independent studies have shown that the scale-invariant measures seem to be superior tools [37]. It should also be noted that the wavelet transform amplitude at a fixed time-scale is closely related to the linear measure SDANN. Substituting the robust standard deviation by a wavelet transform amplitude is a technical fine-tuning which cannot be expected to result in a qualitatively new information.

The multifractal structure of the heart rate signal has several consequences. Thus, the qth-order structure function (a concept borrowed from the theory of the fully-developed turbulence) of the heart rate interval has a scaling behaviour, with the scaling exponent $\zeta(q)$ being a function of q [38]. Note that this spectrum of exponents is very closely related to the above-mentioned $\tau(q)$ spectrum (both describing the same physical phenomenon, differences being of a technical kind). However, the wavelet-transform-based technique makes a more complete utilization of the underlying data and therefore, the $\tau(q)$ spectrum can be expected to yield somewhat superior prognostic and/or diagnostic results.

Another aspect related to the multifractal nature of the heart rhythm is the multi-scale entropy (MSE) [39]. While the single-scale entropies (approximate entropy, Shannon entropy) are related to the short-time dynamics of the heart rhythm and to the probability distribution function of points in the reconstructed phase-space, the MSE extends these concepts to longer time-scales. The MSE is not directly reducible to the multifractal spectra $f(h)$ [or $\tau(q)$]; however, both techniques address the question of how wide is the range of dynamics for the mean heart rate (averaged over a time T), depending on the time-scale T. The clinical usefulness of the MSE is still unclear (apart from the fact that it has been claimed to distinguish between healthy subjects and patients with congestive heart failure [39]).

6. INTERMITTENCY OF HRV

A multifractal spectrum addresses only one aspect of the non-Gaussianity of the time-series increments by revealing the possible range of scaling laws for the long-range [at time-scale of many ($\gg 1$) heartbeat intervals] dynamics of the mean heart rhythm. While the origin of the multifractal scaling is in the intertwining of periods of different variability levels (cf. [12] and Fig. 8), the multifractal spectra fail to reflect all the features of the intertwining phenomena. In particular, this applies to the long-term correlations in the dynamics of short-time variability (which, in effect, does fluctuate in a complex manner). A quantitative scale-invariant analysis of this aspect is based on the distribution law of the low-variability periods [40,41], which will be discussed below. Another aspect of such an intertwining is the clustering of the periods of a similar mean heart rate: the heart rate signal can be divided into segments of a different mean heart rate, with distinct boundaries

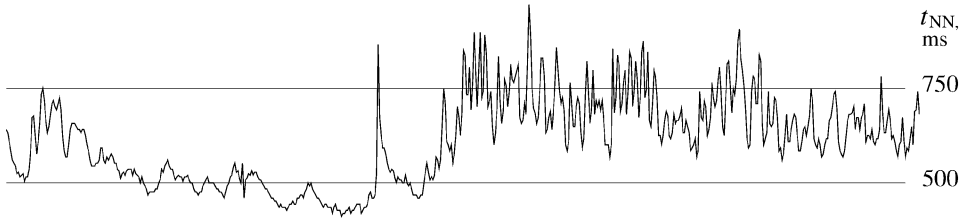

Fig. 8. For healthy patients, the high- and low-variability periods of the heart rhythm are intertwined.

between these segments; there is a power-law segment-length distribution of the segments [42].

In order to analyse quantitatively the intertwining of high- and low-variability periods, we have studied the distribution of low-variability periods and showed that typically, it follows a multiscaling Zipf's law. Originally, Zipf's law has been formulated by G. K. Zipf for the frequency of words in natural languages [43]. For a given language (e.g. English), the frequency (the number of occurrences divided by the total number of words) of each word is calculated on the basis of a large set of texts. The ranks are determined by arranging the words according to their frequency f: the most frequent word obtains rank $r = 1$, the second frequent – $r = 2$, etc. It turns out that for a wide range of ranks (starting with $r = 1$), there is a power law $p(r) \propto r^{-\alpha}$, where $\alpha \approx 1$. This law is universal; it holds for all the natural languages and for a wide variety of texts [43]. Furthermore, similar scaling laws describe the rank-distribution of many other classes of objects as well. Thus, when cities are arranged according to their population s, the population of a city $s \propto r^{-\alpha}$, with $\alpha \approx 1$ [43]. Another example is the income-rank relationship for companies; here we have again $\alpha \approx 1$ [43]. In the most general form, the law can be formulated as $p \propto (r + r_0)^{-\alpha}$, and α is not necessarily close to unity [36]. This more general form of the law can be applied to the distribution of scientists according to their citation index, to the distribution of internet sites according to the number of visitors, etc.

Zipf's law is characteristic of such dynamical systems at statistical equilibrium, which satisfy the following conditions: (a) the system consists of elements of different size; (b) the element size has upper and lower bounds; (c) there is no intermediate intrinsic size for the elements. The human heart rate, when divided into the low-variability periods, satisfies all these requirements. The duration τ of these periods varies in a wide range of scales, from few to several hundreds of heartbeats. Thus, one can expect that the rank-length distribution $r(\tau)$ follows Zipf's law,

$$r \propto \tau^{-\gamma}. \tag{2}$$

First we have to define the local HRV as the deviation of the heart rate from the local average,

$$\delta(n) = [t_{\rm NN}(n) - \langle t_{\rm NN}(n)\rangle]/\,\langle t_{\rm NN}(n)\rangle\,;$$

the local average is calculated using a narrow (≈ 5-second-wide) Gaussian weight-function. Then, the low-variability regions are defined as consecutive sequences of intervals with $|\delta(n)| < \delta_0$; the length τ of such a region is measured as the number of beats in the sequence. Further, all the low-variability regions are numbered (to identify them later), and arranged according to their length; regions of equal length are ordered randomly. In such a way, the longest observed region obtains rank $r = 1$, second longest – $r = 2$, etc. Typically, the length-rank relationship reveals multiscaling properties, i.e. within a certain range of scales, the scaling law (2) is observed, the scaling exponent γ being a (nonconstant) function of the threshold level, $\gamma = \gamma(\delta_0)$ (see Fig. 9).

It is not surprising that the scaling behaviour is not perfect. Indeed, the heart rhythm is a nonstationary signal affected by the nonreproducible daily activities of the subjects. The nonstationary pattern of these activities, together with their time-scales, is directly reflected in the rank-length law. This distribution law can also have a fingerprint of the characteristic time-scale (10 to 20 s) of the blood pressure oscillations (which modulate the level of HRV, cf. [44]). It should be emphasized that the problem of the nonreproducible daily activities affects also the

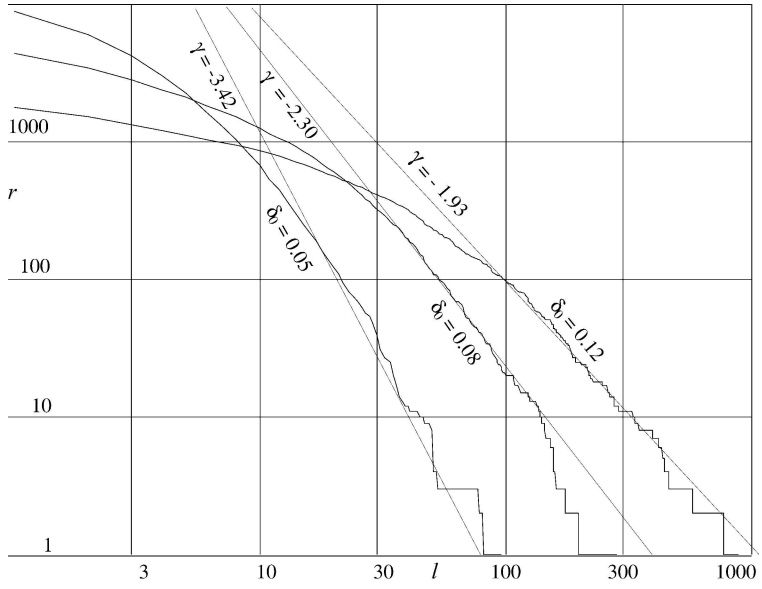

Fig. 9. Multiscaling behaviour: the rank r of low-variability intervals is plotted against the length l of the intervals (measured in the number of heartbeats). The scaling exponent γ depends on the threshold value δ_0.

reliability of the other scale-invariant measures and is probably the main obstacle preventing the clinical application of the seemingly extremely efficient diagnostic and prognostic techniques. Finally, there is a generic reason why Zipf's law is nonperfect at small rank numbers: while Zipf's law is a statistical law, each rank-length curve is based only on a single measurement. In particular, there is only one longest low-variability period (likewise, only one most-frequent word), the length of which is just as long as it happens to be; there is no averaging whatsoever. For large ranks, the relative statistical uncertainty can be estimated as $1/\sqrt{r}$.

The distribution function of the low-variability periods as a whole contains a significant amount of diagnostically valuable information, which is not covered by any other (linear or nonlinear) measure of HRV. The most part of this information seems to be reflected (according to the Student test analysis using the test groups of Table 1) by the parameters τ_{end} (the scale at which the scaling law breaks; for a precise definition, see [41]), $r_{\max}$ (the maximal observed rank), and r_{100} (the rank of the interval with $\tau = 100$; the diagnostical performance of this parameter is similar to that of $r_{\max}$). These measures allow a clear distinction between the healthy subjects and the IHD, VES, and PCI groups [41]; the p-values are presented in Table 3 (for a reference, the data of the two best-performing linear measures are also provided).

Table 3. p-values of the Student test. Data in the topmost triangular region (with label *A*) are calculated using the parameter $\ln \tau_{\text{end}}$ (the logarithmic measure is used to achieve a nearly-Gaussian data distribution). Triangular region *B* corresponds to the parameter $\ln r_{\max}$, region *C* – to the linear measure pnn50, and region *D* – to the linear measure SDNN. Since multiple tests were carried out, modified Bonferroni correction [45] has to be applied. Grey background highlights the tests with the adjusted significance $p' < 10\%$. The control parameter value $\delta_0 = 0.05$ has been used

p, %	Healthy	IHD	SND	VES	PCI	RR
Healthy	*B* / *A*	0.06	17.21	0.02	0.07	1.59
IHD	0.36		2.85	96.79	97.62	21.93
SND	2.99	59.10		2.10	3.04	25.77
VES	0.08	91.60	63.79		94.18	17.59
PCI	25.27	21.61	46.37	22.89		22.50
RR	0.14	73.57	77.69	80.49	28.90	
Healthy	*D* / *C*	7.01	10.01	0.01	0.98	4.34
IHD	3.89		2.70	45.88	62.20	74.98
SND	0.64	0.10		1.44	3.40	3.23
VES	8.83	64.71	0.15		3.46	16.26
PCI	14.93	0.99	3.31	1.98		12.63
RR	21.58	1.07	1.94	2.38	70.25	

7. MODE-LOCKING BETWEEN THE HEART RHYTHM AND RESPIRATION

As mentioned above, respiration affects (modulates) the heart rhythm. This effect is mediated by the blood pressure, and the effect known as baroreflex (heart rhythm depends on the blood pressure). The heart is most responsive with respect to the signals of the autonomous nervous system when the heart rate is slow, i.e. when the patient is at rest. In that case, HRV is driven by weaker signals, like the signals induced by respiration, which (due to their quasi-periodic nature) may lead to a mode-locking. In the case of mode-locking, the heart rate is automatically slightly adjusted so that the respiration and heart beat periods relate to each other as (small) integers. As a result, the decorrelation time between the heart rhythm and respiration can be very long. This is the effect which is in most cases the cause of the patterns (isolated clouds of points) observable in the reconstructed phase space (see Fig. 3).

The mode-locking has been studied using bivariate data (simultaneous ECG and respiration data) and the technique called cardiorespiratory synchrogram [44]. Also, a univariate data analysis method using the angle-of-returntime map has been elaborated [46]. In that case, the data-set is used to reconstruct the phase of forcing (breathing) and the phase of oscillator (heart). These phases are plotted versus each other; in the case of mode-locking, disjoint clouds of points will appear.

Recently, we have developed an independent, intuitive and easy to use method of mode-locking detection from univariate data (RR-interval sequence), which is based on analysis of the fluctuation function $F(\nu)$, defined by Eq. (1) [24]. The fluctuation function of the patients with mode-locking revealed the presence of an oscillatory component, see Fig. 10b. By dividing the entire 24-hour HRV record into one-hour intervals, and calculating the amplitude of the oscillatory component (via a wavelet transform) of the fluctuation function for each interval, we were able to locate the periods responsible for the satellite clouds in the reconstructed phase-space. These were always the periods before falling asleep, around 10 or 11 pm, characterized by a low heart rate and a high respiration-driven short-time variability. The phase between the heart rate and respiration is locked during tens of seconds, confirming the observations of Schäfer et al. [44]. Thus, in a certain sense, the heart and respiratory complex act as a system of coupled oscillators. Finally we note that a specific feature of the patients with strong mode-locking was the presence of well-defined "satellite clouds" in time-delay map (see Fig. 3). Therefore, the time-delay map can be also used to detect mode-locking; however, this method is nonquantitative, less sensitive than the fluctuation-function-based technique, and does not give a hint which mode-locking modes are observed. The presence of a natural quantitative measure (the wavelet transform amplitudes) is also the main advantage of our approach over the alternative method.

As compared with the alternative techniques, our method of mode-locking detection is very simple and does not require synchronous respiration rhythm recording (unlike the thorough method [44]), and can be conveniently used to find

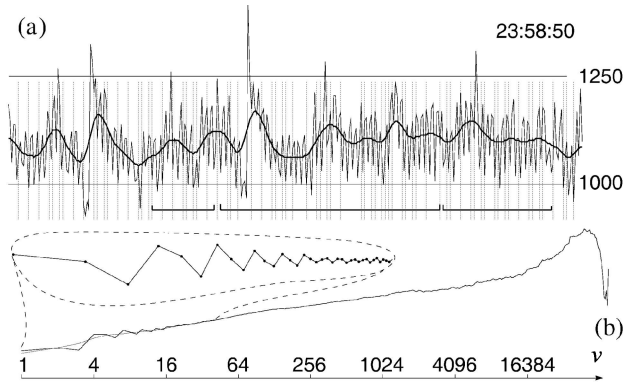

Fig. 10. Patient with 3:1 mode-locking between the heart rate and respiration: (a) heartbeat intervals (in milliseconds) plotted versus the beat number. The heart rate has a pronounced oscillatory component; vertical lines mark the period of three heartbeats, horizontal lines indicate the sequences with coherent phase. (b) Fluctuation function (arbitrary units) is plotted versus the time lag ν (in heartbeats); the oscillating component is magnified.

relatively short ($\gtrsim$ 10 min) locking periods from a 24-hour recording. Besides, it provides a natural measure to quantify the degree of mode-locking (unlike the method of using the angle-of-returntime map [46]).

8. CONCLUSIONS

Below is an attempt to classify the measures of heart rate variability.

1. "Classical" linear methods – based on standard statistical measures and on the Fourier analysis. These are the only methods widely used in clinical practice.
2. "New" linear methods: wavelet spectra.
3. Nonlinear methods:
   (a) scale-invariant methods:
      i. single-scaling analysis (calculation of the Hurst exponent H);
      ii. multi-scaling analysis – calculation of the exponent spectra [Lipschitz–Hölder spectrum $f(h)$, mass exponents $\tau(q)$, or structure function exponent spectrum $\zeta(q)$]; these seem to be the most promising measures, at least for prognostic purposes;
      iii. calculation of the multiscale entropy;
      iv. analysis of the HRV-data segments with a similar mean heart rate;
      v. analysis of the distribution law of low-variability periods (performs well in diagnostic tests, there are no prognostic tests yet);
   (b) scale-dependent methods:
      i. performing a phase-space analysis (entropy-based measures, correlation dimension, Lyapunov exponents, etc.);
      ii. heart rhythm and respiration mode-locking analysis.

The human heart rate fluctuates in a complex and nonstationary manner. Elaborating efficient and adequate tools for the analysis of such signals has been a great challenge for the researchers during last decades. The above long list of nonlinear techniques proves that the research has been successful and various important features of such time-series have been revealed. Nevertheless, there is no consensus of which methods are the most efficient ones from the point of view of clinical applications. On the one hand, this is caused by the high nonstationarity and irreproducibility of these time-series: the complex measures of HRV depend not only on the healthiness of the heart, but also on the daily habits of the subject [47] and on the random events of the recording day. On the other hand, dialogue between physicists and doctors seems to be inefficient: physicists publish research results based on small test groups; doctors are waiting for follow-up studies using extended and homogeneous test groups. However, the situation is expected to start improving, owing to the new projects bringing together medical doctors and physicists (cf. http://www.physionet.org).

ACKNOWLEDGEMENT

This study was supported by the Estonian Science Foundation (grant No. 4151).

REFERENCES

1. Liebovitch, L. S., Todorov, A. T., Zochowski, M., Scheurle, D., Colgin, L., Wood, M. A., Ellenbogen, K. A., Herre, J. M. and Bernstein, R. C. Nonlinear properties of cardiac rhythm abnormalities. *Phys. Rev. E*, 1999, **59**, 3312–3319.
2. Lass, J. *Biosignal Interpretation: Study of Cardiac Arrhythmias and Electromagnetic Field Effects on Human Nervous System*. PhD theses, TTU Press, 2002.
3. Hon, E. H. and Lee, S. T. Electronic evaluations of the fetal heart rate patterns preceding fetal death, further observations. *Am. J. Obstet. Gynec.*, 1965, **87**, 814–826.
4. Wolf, M. M., Varigos, G. A., Hunt, D. and Sloman, J. G. Sinus arrhythmia in acute myocardial infarction. *Med. J. Australia*, 1978, **2**, 52–53.
5. Akselrod, S., Gordon, D., Ubel, F. A., Shannon, D. C., Barger, A. C. and Cohen, R. J. Power spectrum analysis of heart rate fluctuation: a quantitative probe of beat to beat cardiovascular control. *Science*, 1981, **213**, 220–222.
6. Kleiger, R. E., Miller, J. P., Bigger, J. T., Moss, A. J. and the Multi-center Post-Infarction Research Group. Decreased heart rate variability and its association with increased mortality after acute myocardial infarction. *Am. J. Cardiol.*, 1987, **59**, 256–262.
7. Malik, M., Farrell, T., Cripps, T. and Camm, A. J. Heart rate variability in relation to prognosis after myocardial infarction: selection of optimal processing techniques. *Eur. Heart J.*, 1989, **10**, 1060–1074.
8. Bigger, J. T., Fleiss, J. L., Steinman, R. C., Rolnitzky, L. M., Kleiger, R. E. and Rottman, J. N. Frequency domain measures of heart period variability and mortality after myocardial infarction. *Circulation*, 1992, **85**, 164–171.
9. West, B. J., Goldberger, A. L., Rooner, G. and Bhargava, V. Nonlinear dynamics of the heartbeat. 1. The av junction: passive conduct on active oscillator. *Physica D*, 1985, **17**, 198–206.

10. Engelbrecht, J. and Kongas, O. Driven oscillators in modelling of heart dynamics. *Appl. Anal.*, 1995, **57**, 119–144.
11. Babloyantz, A. and Destexhe, A. Is the normal heart a periodic oscillator? *Biol. Cybern.*, 1988, **58**, 203–211.
12. Poon, C. S. and Merrill, C. K. Decrease of cardiac chaos in congestive heart failure. *Nature*, 1997, **389**, 492–495.
13. Voss, A., Kurths, J., Kleiner, H. J., Witt, A., Wessel, N., Saparin, P., Osterziel, K. J., Schurath, R. and Dietz, R. The application of methods of non-linear dynamics for the improved and predictive recognition of patients threatened by sudden cardiac death. *Cardiovasc. Res.*, 1996, **31**, 419–433.
14. Pincus, S. Approximate entropy (ApEn) as a complexity measure. *Chaos*, 1995, **5**, 110–117.
15. Govindan, R. B., Narayanan, K. and Gopinathan, M. S. On the evidence of deterministic chaos in ECG: surrogate and predictability analysis. *Chaos*, 1998, **8**, 495–502.
16. Grassberger, P. and Procaccia, J. Measuring the strangeness of a strange attractor. *Physica D*, 1983, **9**, 189–208.
17. Kantz, H. and Schreiber, T. Dimension estimates and physiological data. *Chaos*, 1995, **5**, 143–154.
18. Kanters, J. K., Holstein-Rathlou, N. H. and Agner, E. Lack of evidence for low-dimensional chaos in heart rate variability. *J. Cardiovasc. Electrophys.*, 1994, **5**, 591–601.
19. Bezerianos, A., Bountis, T., Papaioannou, G. and Polydoropoulus, P. Nonlinear time series analysis of electrocardiograms. *Chaos*, 1995, **5**, 95–101.
20. Berne, R. M. and Levy, N. M. *Cardiovascular Physiology*. Eighth edition. Mosby, New York, 2001.
21. Kaplan, D. L. and Talajic, M. Dynamics of heart rate. *Chaos*, 1991, **1**, 251–256.
22. Rosenblum, M. and Kurths, J. A model of neural control of the heart rate. *Physica A*, 1995, **215**, 439–450.
23. Kantz, H. and Schreiber, T. *Nonlinear Time Series Analysis*. Cambridge University Press, 1997.
24. Säkki, M., Kalda, J., Vainu, M. and Laan, M. What does measure the scaling exponent of the correlation sum in the case of human heart rate? *Chaos*, 2004, **14**, 138–144.
25. Zebrowski, J. J., Poplawska, W., Baranowski, R. and Buchner, T. Symbolic dynamics and complexity in a physiological time series. *Chaos, Solitons, Fractals*, 2000, **11**, 1061–1075.
26. Peng, C. K., Mietus, J., Hausdorff, J. M., Havlin, S., Stanley, H. E. and Goldberger, A. L. Long-range anticorrelations and non-Gaussian behavior of the heartbeat. *Phys. Rev. Lett.*, 1993, **70**, 1343–1347.
27. Peng, C. K., Havlin, S., Stanley, H. E. and Goldberger, A. L. Quantification of scaling exponents and crossover phenomena in nonstationary heartbeat time series. *Chaos*, 1995, **5**, 82–87.
28. Ivanov, P. Ch., Rosenblum, M. G., Amaral, L. A. N., Struzik, Z., Havlin, S., Goldberger, A. L. and Stanley, H. E. Multifractality in human heartbeat dynamics. *Nature*, 1999, **399**, 461–465.
29. Amaral, L. A. N., Goldberger, A. L., Ivanov, P. Ch. and Stanley, H. E. Scale-independent measures and pathologic cardiac dynamics. *Phys. Rev. Lett.*, 1998, **81**, 2388–2391.
30. Thurner, S., Feurstein, M. C. and Teich, M. C. Multiresolution wavelet analysis of heartbeat intervals discriminates healthy patients from those with cardiac pathology. *Phys. Rev. Lett.*, 1998, **80**, 1544–1547.
31. Mandelbrot, B. B. and Van Ness, J. V. Fractional Brownian motion, fractional noises and applications. *SIAM Rev.*, 1968, **10**, 422–434.

32. Kobayashi, M. and Musha, T. $1/f$ fluctuation of heart beat period. *IEEE Trans. Biomed. Eng.*, 1982, **29**, 456–457.
33. Yamamoto, Y. and Hughson, R. L. Coarse-graining spectral analysis: new method for studying heart rate variability. *J. Appl. Physiol.*, 1991, **71**, 1143–1150.
34. Ashkenazy, Y., Lewkowicz, M., Levitan, J., Havlin, S., Saermark, K., Moelgaard, H. and Bloch Thomsen, P. E. Discrimination of the healthy and sick cardiac autonomic nervous system by a new wavelet analysis of heartbeat intervals. *Fractals*, 1999, **7**, 85–91.
35. Ashkenazy, Y., Lewkowicz, M., Levitan, J., Moelgaard, H., Bloch Thomsen, P. E. and Saermark, K. Discrimination of the healthy and sick cardiac autonomic nervous system by a new wavelet analysis of heartbeat intervals. *Fractals*, 1998, **6**, 197–203.
36. Mandelbrot, B. B. *The Fractal Geometry of Nature*. Freeman, San Francisco, 1983.
37. Saermark, K., Moellery, M., Hintzey, U., Moelgaardz, H., Bloch Thomsenx, P. E., Huikuri, H., Makikiallio, T., Levitan, J. and Lewkowicz, M. Comparison of recent methods of analyzing heart rate variability. *Fractals*, 2000, **8**, 315–322.
38. Lin, D. C. and Hughson, R. L. Modeling heart rate variability in healthy humans: a turbulence analogy. *Phys. Rev. Lett.*, 2001, **86**, 1650–1653.
39. Costa, M., Goldberger, A. L. and Peng, C.-K. Multiscale entropy analysis of complex physiologic time series. *Phys. Rev. Lett.*, 2002, **89**, 068102 (4 pages).
40. Kalda, J., Vainu, M. and Säkki, M. The methods of nonlinear dynamics in the analysis of heart rate variability for children. *Med. Biol. Eng. Comp.*, 1999, **37**, 69–72.
41. Kalda, J., Säkki, M., Vainu, M. and Laan, M. Zipf's law in human heartbeat dynamics. *e-print* http://arxiv.org/abs/physics/0110075, 2001 (4 pages).
42. Bernaola-Galván, P., Ivanov, P. Ch., Amaral, L. A. N. and Stanley, H. E. Scale invariance in the nonstationarity of human heart rate. *Phys. Rev. Lett.*, 2001, **87**, 168105 (4 pages).
43. Zipf, G. K. *Human Behavior and the Principle of Least Effort*. Addison-Wesley, Cambridge, 1949.
44. Schäfer, C., Rosenblum, M. G., Kurths, J. and Abel, H. H. Heartbeat synchronized with ventilation. *Nature*, 1998, **392**, 239–240.
45. Jaccard, J. and Wan, C. K. *LISREL Approaches to Interaction Effects in Multiple Regression*. Sage Publications, Thousand Oaks, CA, 1996.
46. Janson, N. B., Balanov, A. G., Anishchenko, V. S. and McClintock, P. V. E. Phase synchronization between several interacting processes from univariate data. *Phys. Rev. Lett.*, 2001, **86**, 1749–1752.
47. Struzik, Z. R. Revealing local variability properties of human heartbeat intervals with the local effective Hölder exponent. *Fractals*, 2001, **9**, 77–93.

Mittelineaarne ja mastaabi-invariantne südamerütmi muutlikkuse analüüs

Jaan Kalda, Maksim Säkki, Meelis Vainu ja Mari Laan

Inimese südamerütm fluktueerub keerulisel ja mittestatsionaarsel moel. Efektiivsete ja seda tüüpi ajajadade jaoks adekvaatsete analüüsimeetodite väljatöötamine on viimaste aastakümnete jooksul olnud teadlastele tõsiseks väljakutseks. Käesolevas ülevaates käsitletakse selles valdkonnas saavutatud põhitulemusi. Pearõhk pannakse küsimustele, millised on südamerütmi ajajada olulisimad eriomased jooned ja millised on diagnostiliste ja prognostiliste rakenduste seisukohast kõige perspektiivikamad mittelineaarsed rütmimuutlikkuse mõõdud.